

Functional Roles of Ionic Currents in a Membrane Delimited Mouse Sino-atrial Node Model

S Kharche, J Higham, M Lei, H Zhang

School of Physics and Astronomy, University of Manchester, Manchester, UK

Abstract

Functional roles of ionic currents in a membrane delimited sino-atrial node (SAN) cell model were investigated. Ionic currents were blocked and intracellular calcium ($[Ca^{2+}]_i$) buffered to study their effects on action potential (AP) characteristics.

The simulations revealed that blocking the hyperpolarization activated current and the T-type calcium current caused an increase of cycle length (CL) due to reduced diastolic depolarization rate (DDR). Blocking of sustained outward (I_{s1}) and sodium currents ($I_{Na,1.1}$, $I_{Na,1.5}$) had no effect. Blocking the L-type calcium current's $Ca_v1.3$ isoform ($I_{CaL1.3}$) and rapidly activating delayed rectifier arrested pacemaking. Blocking sodium-calcium exchanger (I_{NaCa}) caused a CL reduction but did not affect DDR. Reducing $[Ca^{2+}]_i$ increased CL marginally. A small increase of $[Ca^{2+}]_i$ arrested pacemaking. I_{sb} , $I_{Na,1.1}$, and $I_{Na,1.5}$ are not functional and I_{NaCa} is a background current in the model.

1. Introduction

Modelling of electrical action potentials (APs) in cardiac cells started with early models by Nobel et al. [1] which incorporated the gross function of depolarising and repolarising cell membrane ionic currents. With the increasing availability of quantitative physiological data suitable for modelling, several generations of models are now capable of reproducing electrical heterogeneity in various cardiac cell types, e.g. see [2-4], and are often specific to species, e.g. see [2, 5, 6]. Cardiac models are ideal *in silico* computational tools for confirming experimental findings [7], hypotheses testing [8], and are also used in predictive studies [9].

Contemporary cell models are systems of stiff non-linear coupled ordinary differential equations (ODEs) and consist of compartmental models of cell membrane ionic currents and intracellular ion concentration dynamics. The complex interaction between the ionic currents and intracellular dynamics regulates the cell membrane AP profile and AP duration (APD). Biophysical parameters

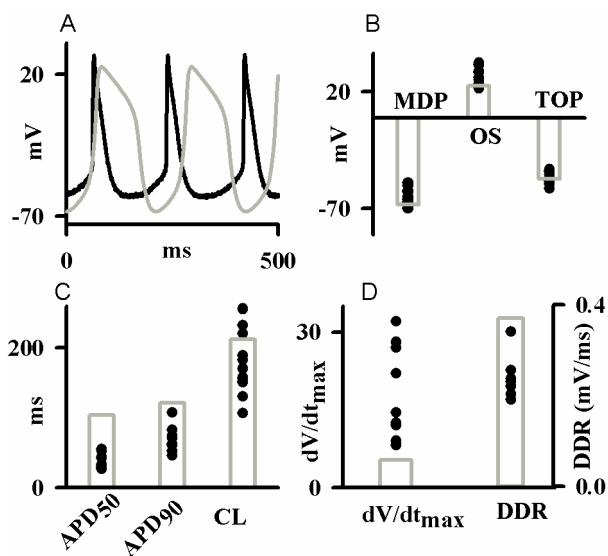


Figure 1 Simulated and experimental AP profiles and AP characteristics, where solid line and symbols show experimental data and gray line and columns show model simulation. A: Representative experimental and simulated AP profiles. B: Experimental data and simulated values for MDP, OS and TOP of the spontaneous APs. C: Experimental data and simulated values for APD₅₀, APD₉₀ and CL of the spontaneous APs. D: dV/dt_{max} and DDR.

in these models should be based on experimental data. Such physiological experimental data quantifying the biophysical processes are however often limited or unavailable. The models therefore borrow data from other tissue types, species, or are estimated by biophysical and physiological motivations [10]. Often the limited data leads to a class of membrane delimited models in which intracellular ionic concentrations are assumed constant at diastolic levels [2, 5]. Such an approximation may be justified due to the small oscillation amplitudes of intracellular ionic concentrations. It also reduces the computational complexity. It however, limits model functionality. Membrane delimited models cannot

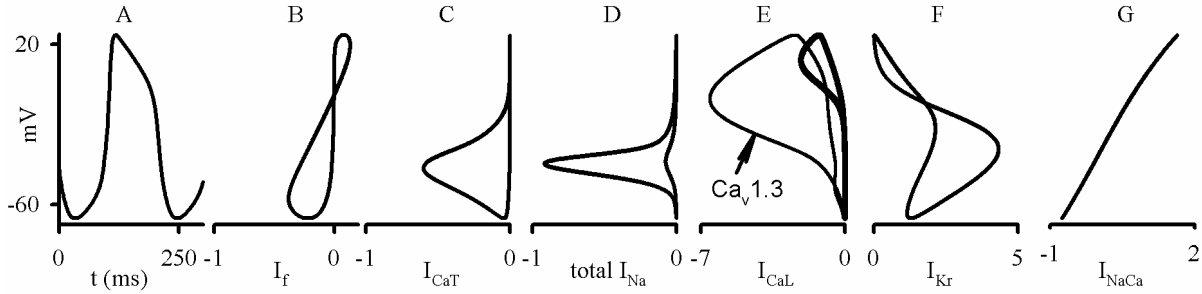


Figure 2 Phase planes of major currents (nA) with respect to membrane potential revealing the maximal functional roles of the currents during a typical AP excitation. A: AP. B: I_f . C: I_{CaT} . D: I_{Na} . E: I_{CaL} ($I_{CaL,1.2}$ and $I_{CaL,1.3}$). F: I_{Kr} . G: I_{NaCa} .

be used in the study of intracellular ionic dynamics based regulation of membrane APs, as has been demonstrated in recent experimental studies of intracellular calcium ($[Ca^{2+}]_i$) based pacemaking mechanisms of the sino-atrial node (SAN) [11, 12]. In addition, the computational estimation of ionic currents for which experimental data is unavailable is based only on AP profiles without recourse to material balance and sensibility of intracellular ion concentration oscillations.

In this study, we studied one such model of the mouse SAN spontaneous APs by Mangoni et al. [13]. The functional role of individual ionic currents in the pacemaking mechanisms was studied by physiological experiment motivates simulation of altered ionic current conductances in the model and its effects on AP characteristics.

2. Methods

The Mangoni et al. [13] model simulates spontaneous SAN pacemaker APs in the mouse SAN. Features of APs were quantified by measuring maximum diastolic potential (MDP), take off potential (TOP), overshoot potential (OS), AP amplitude (APA), APD at 50% repolarisation (APD_{50}), APD at 90% repolarisation (APD_{90}), cycle length (CL), upstroke velocity (dV/dt_{max}), and diastolic depolarisation rate (DDR) [14]. The model consists of several cell membrane ionic currents regulating cell membrane potential, V , dynamics as

$$C_m \frac{dV}{dt} = -(I_f + I_{st} + I_{CaT} + I_{Na,1.1} + I_{Na,1.5} + I_{CaL,1.2} + I_{CaL,1.3} + I_{to} + I_{sus} + I_{Ks} + I_{Kr} + I_{K1} + I_{NaCa} + I_{NaK} + I_b) \quad \text{eq. (1)}$$

where the hyperpolarisation activated current (I_f), the sustained outward Ca^{2+} current (I_{st}), T-type Ca^{2+} current (I_{CaT}) regulate the slow diastolic depolarisation rate (DDR); the fast sodium current isoforms (TTX sensitive $I_{Na,1.1}$ and TTX resistant $I_{Na,1.5}$), the L-type Ca^{2+} isoforms ($I_{CaL,1.2}$ and $I_{CaL,1.3}$) regulate the AP upstroke phases; the

transient outward (I_{to}), the sustained outward (I_{sus}), the slow and rapidly activating (I_{Ks} and I_{Kr}), and the inward rectifier (I_{K1}) K^+ currents regulate the AP repolarisation; and the Na^+ - Ca^{2+} exchanger (I_{NaCa}) and the Na-K pump (I_{NaK}) are background currents along with I_b . C_m is cell membrane capacitance of 21 pF. Intracellular concentrations of $[Ca^{2+}]_i$, $[K^+]_i$ and $[Na^+]_i$ are constant at 0.1 μM , 8 mM and 140 mM respectively as given in the basal model [13]. Values of ion current conductances and maximal values are given in the model [13]. Basal spontaneous AP profile and AP characteristics are compared to experimental data in Figure 1. The action of the major currents during various regions of the AP in the basal model was identified by means of phase plane analysis as shown in Figure 2.

The role of ionic currents on the pacemaking AP was evaluated by altering ionic current conductances of each ionic current from a 100% reduction to a 400% increase. Such changes in conductances simulated the partial and total experimental blocking of the ionic currents by various concentrations of pharmacological agents. Further, the influence of intracellular concentrations quantified by systematically varying the constant $[Ca^{2+}]_i$ between 0.0001 μM to 0.3 μM . The effects of the conductance and $[Ca^{2+}]_i$ alterations on the pacemaking APs were quantified by computing changes in AP characteristics as discussed above. Model behaviour was compared to available experimental data.

The model was integrated using a Quality Step Runge-Kutta method with a maximal time step of 0.25 ms in XPPAUT/AUTO software [15]. A total of 20 s of electrical activity were simulated for each value of conductance or intracellular concentration to eliminate the transient effects of the initial conditions, and AP characteristics computed for the final 1 s. The integration was systematically repeated from the lowest to the largest values of each parameter in steps of 2.5% change in value of parameter, to give continuous changes in AP characteristics. A Linux shell script wrapper was implemented to automate the silent mode XPPAUT simulations.

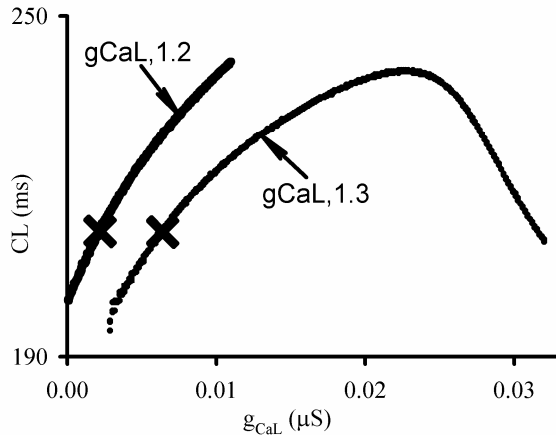


Figure 3 Effects of perturbing $I_{CaL,1.2}$ and $I_{CaL,1.3}$ amplitude by manipulating $g_{CaL,1.2}$ and $g_{CaL,1.3}$ on pacemaking CL. The 'X' show basal values of $g_{CaL,1.2}$ and $g_{CaL,1.3}$.

3. Results

As seen in Figure 1, several basal model AP characteristics agree well with experimental data. The model has an MDP of -66.8 mV, an OS of 24.6 mV, and a TOP of -47.3 mV. Model APD_{50} and APD_{90} , 104 ms and 121 ms respectively, are significantly longer than experimentally observed range of values. Model CL is 212.3 ms. The model produces a dV/dt_{max} of 5.3 mV/ms, which is lower than experimental values. Model simulated DDR of 0.37 V/s is much larger than experimental observations, and is due to the long APD. The phase space diagrams in Figure 2 show the region of the AP profiles in which major currents are active.

The functional currents in the DDR region of the AP are I_f , I_{st} and I_{CaT} . A total block of I_f increased the CL by 10.3% (234.9 ms). Blocking I_{st} had an insignificant effect on the AP. Blocking I_{CaT} caused a 6.1% increase of CL, as compared to the tissue level recording of 34% in $Ca_v3.1$ gene knockout mice [13]. The functional currents in the upstroke and APD region are $I_{Na,1.1}$, $I_{Na,1.5}$, $I_{CaL,1.2}$ and $I_{CaL,1.3}$. Blocking of $I_{Na,1.1}$ and $I_{Na,1.5}$ in the model had no effect on the pacemaking AP. This is in contrast to our experimental measurements where a large increase of CL of more than 30% was observed on isolated mouse SAN cells with $SCN5A$ gene knockout [16]. As seen in Figure 3, progressive reduction of $I_{CaL,1.2}$ and $I_{CaL,1.3}$ increased the pacemaking rate, by reducing the CL. A total block of $I_{CaL,1.2}$ gave a CL reduction of 6%, while a block of $I_{CaL,1.3}$ arrested the pacemaking. Upon progressively increasing $I_{CaL,1.2}$ and $I_{CaL,1.3}$, the CL was seen to increase. In case of $I_{CaL,1.3}$, CL eventually reduced and oscillation became chaotic. It should be noted that the increased pacemaking due to I_{CaL} block was accompanied by reduced oscillation strength (i.e. a reduced APA) indicating the regulatory contribution of I_{CaL} to the pacemaking. I_{Kr} is the main

repolarising current in the SAN, and as seen in Figure 4, a block of I_{Kr} abolished pacemaking. It did not affect the pacemaking as it was progressively augmented. Eventually, for very large values of I_{Kr} , the AP became chaotic. I_{NaCa} has been experimentally shown to be critical in SAN pacemaking and regulates the DDR phase [8]. In the present model however, I_{NaCa} has low amplitude. A total block of I_{NaCa} increased the CL modestly by 18%, while a large increase of I_{NaCa} amplitude by 400% reduced the CL by 9%. Both these effects are modest. Further, contrary to experimental findings [17], a large reduction of $[Ca^{2+}]_i$ (from 0.1 μ M to 0.0001 μ M) increased APA and reduced the CL by less than 7%. A modest increase of $[Ca^{2+}]_i$ (from 0.1 μ M to 0.2 μ M) abolished pacemaking activity.

Figure 5 shows a summary of the effects of individually blocking each current on the pacemaking.

4. Conclusions and discussion

Although several membrane currents have been incorporated into the model, the roles of each current is limited. Major currents like I_{st} , $I_{Na,1.1}$ and $I_{Na,1.5}$ do not play any role in the pacemaking APs of the model. Due to the model being inherently membrane delimited,

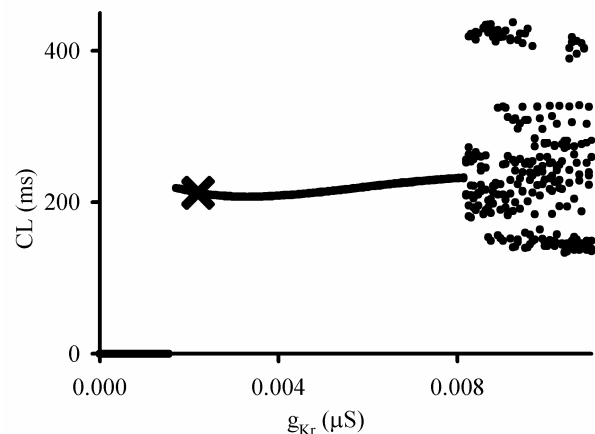


Figure 4 Effects of reducing and increasing I_{Kr} on pacemaking CL. The 'X' show basal values of g_{Kr} . For large values of g_{Kr} , the oscillations became chaotic.

mechanism by which critical currents like I_{NaCa} contribute to the DDR cannot be incorporated into the model. This has led the I_{NaCa} in the present model act as a simple background current with modest effects on the pacemaking. Experimentally, a reduced intracellular $[Ca^{2+}]_i$ reduced pacemaking strength, and a low concentrations abolishes automaticity. In contrast, the model shows no change in pacemaking with a reduced $[Ca^{2+}]_i$, but contrarily shows an increase of APA. This is due to the $[Ca^{2+}]_i$ not contributing to I_{CaL} inactivation and

other mechanisms dynamically.

The model is an excellent simulation tool for preliminary evaluation of experimental data. It is however limited in ability to reproduce experimental findings and in its predictive power.

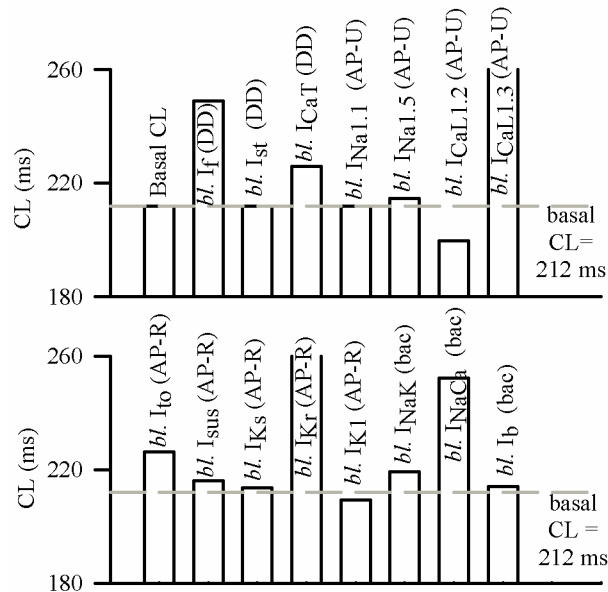


Figure 5 Summary of the effects of channel blocking on CL in the model. Top panel shows the depolarising currents, while the bottom panel shows repolarising and background currents.

Acknowledgements

This work was funded by a Wellcome Trust (UK) grant (WT/081809/Z/06/Z).

References

- [1] Noble D. A modification of the Hodgkin--Huxley equations applicable to Purkinje fibre action and pace-maker potentials. *J Physiol.* 1962; 160:317-52.
- [2] Zhang H, Holden AV, Kodama I, Honjo H, Lei M, Varghese T, et al. Mathematical models of action potentials in the periphery and center of the rabbit sinoatrial node. *Am J Physiol Heart Circ Physiol.* 2000; 279(1):H397-421.
- [3] Lindblad DS, Murphey CR, Clark JW, Giles WR. A model of the action potential and underlying membrane currents in a rabbit atrial cell. *Am J Physiol.* 1996; 271(4 Pt 2):H1666-96.
- [4] Inada S, Hancox JC, Zhang H, Boyett MR. One-dimensional mathematical model of the atrioventricular node including atrio-nodal, nodal, and nodal-his cells. *Biophys J.* 2009; 97(8):2117-27.
- [5] Mangoni ME, Couette B, Marger L, Bourinet E, Striessnig J, Nargeot J. Voltage-dependent calcium channels and cardiac pacemaker activity: from ionic currents to genes. *Prog Biophys Mol Biol.* 2006; 90(1-3):38-63.
- [6] Himeno Y, Sarai N, Matsuoka S, Noma A. Ionic mechanisms underlying the positive chronotropy induced by beta1-adrenergic stimulation in guinea pig sinoatrial node cells: a simulation study. *J Physiol Sci.* 2008; 58(1):53-65.
- [7] Salle L, Kharche S, Zhang H, Brette F. Mechanisms underlying adaptation of action potential duration by pacing rate in rat myocytes. *Prog Biophys Mol Biol.* 2008; 96(1-3):305-20.
- [8] Maltsev VA, Lakatta EG. Synergism of coupled subsarcolemmal Ca²⁺ clocks and sarcolemmal voltage clocks confers robust and flexible pacemaker function in a novel pacemaker cell model. *Am J Physiol Heart Circ Physiol.* 2009; 296(3):H594-615.
- [9] Sachse FB, Moreno AP, Seemann G, Abildskov JA. A model of electrical conduction in cardiac tissue including fibroblasts. *Ann Biomed Eng.* 2009; 37(5):874-89.
- [10] Niederer SA, Fink M, Noble D, Smith NP. A meta-analysis of cardiac electrophysiology computational models. *Exp Physiol.* 2009; 94(5):486-95.
- [11] Chen B, Wu Y, Mohler PJ, Anderson ME, Song LS. Local control of Ca²⁺-induced Ca²⁺ release in mouse sinoatrial node cells. *J Mol Cell Cardiol.* 2009; 47(5):706-15.
- [12] Wu Y, Gao Z, Chen B, Koval OM, Singh MV, Guan X, et al. Calmodulin kinase II is required for fight or flight sinoatrial node physiology. *Proc Natl Acad Sci U S A.* 2009; 106(14):5972-7.
- [13] Mangoni ME, Traboulsie A, Leoni AL, Couette B, Marger L, Le Quang K, et al. Bradycardia and slowing of the atrioventricular conduction in mice lacking CaV3.1/alpha1G T-type calcium channels. *Circ Res.* 2006; 98(11):1422-30.
- [14] Mangoni ME, Nargeot J. Properties of the hyperpolarization-activated current (I_f) in isolated mouse sino-atrial cells. *Cardiovasc Res.* 2001; 52(1):51-64.
- [15] Ementrou B. Simulating, analyzing, and animating dynamical systems: a guide to XPPAUT for Researchers and Students. Philadelphia: SIAM; 2002.
- [16] Lei M, Jones SA, Liu J, Lancaster MK, Fung SS, Dobrzynski H, et al. Requirement of neuronal- and cardiac-type sodium channels for murine sinoatrial node pacemaking. *J Physiol.* 2004; 559(Pt 3):835-48.
- [17] Nikmaram MR, Liu J, Abdelrahman M, Dobrzynski H, Boyett MR, Lei M. Characterization of the effects of ryanodine, TTX, E-4031 and 4-AP on the sinoatrial and atrioventricular nodes. *Prog Biophys Mol Biol.* 2008; 96(1-3):452-64.

Address for correspondence.

Name: Dr. Sanjay Kharche

Full postal address: School of Physics and Astronomy, University of Manchester, Manchester, UK, M13 9PL

E-mail address: Sanjay.Kharche@manchester.ac.uk